

commendable while such models for forests by Indian groups are lacking. Recently, a collaborative attempt was made by the authors with the G.B. Pant National Institute of Himalayan Environment and Sustainable Development, Almora, India, and the York University, and the Ontario Tech University, Canada to develop a dynamic model for the Indian Chir pine (*Pinus roxburghii*) – the PhenoPine¹³, that can be used to trace the phenological changes in Chir pine in response to ambient temperature rise. The PhenoPine is an initial module of the DGVM that we plan to develop as a full-fledged model for the pine-dominant landscape. In due course, we wish to develop models for other dominant and mixed forests that could be coupled with the climate models to assess the response of forests under projected climate change scenarios at regional to global scales.

- Jiang, L., Huang, X., Wang, F., Liu, Y., and An, P., *Ecol. Indic.*, 2018, **85**, 479–486

- Kumar, M., Singh, H., Pandey, R., Singh, M. P., Ravindranath, N. H. and Kalra, N., *Biodivers. Conserv.*, 2019, **28**, 2163–2182.
- Peng, C., *Ecol. Modell.*, 2000, **135**, 33–54.
- Long, S. P., *In Silico Plants*, 2019, **1**, 1–3.
- Kumar, M., Rawat, S. P. S., Singh, H., Ravindranath, N. H. and Kalra, N., *Indian J. For.*, 2018, **41**, 1–12.
- Blanco, J. A., de Andrés, E. G., San Emeterio, L. and Lo, Y.-H., *In Developments in Environmental Modelling*, Elsevier, 2015, pp. 189–215.
- Kucharik, C. J. et al., *Glob. Biogeochem. Cycles*, 2000, **14**, 795–825.
- Foley, J. A. et al., *Global Biogeochem. Cycles*, 1996, **10**, 603–628.
- Sitch, S. et al., *Glob. Chang. Biol.*, 2003, **9**, 161–185.
- Chaturvedi, R. K. et al., *Mitig. Adapt. Strateg. Glob. Chang.*, 2011, **16**, 119–142.
- Aggarwal, P. K., Kalra, N., Chander, S. and Pathak, H., *Agric. Syst.*, 2006, **89**, 1–25.
- Kalra, N. and Kumar, M., In *Climate Change and Agriculture in India: Impact and Adaptation*, 2019, pp. 21–28.
- Kumar, M. et al., *Ecol. Modell.*, 2019, **404**, 12–20.

Received 17 July 2019; revised accepted 4 November 2019

MANOJ KUMAR^{1,*}
NAVEEN KALRA²
N. H. RAVINDRANATH³

¹GIS Centre, IT&GIS Discipline,

Forest Research Institute,

PO: New Forest,

Dehradun 248 006, India

²Division of Agriculture Physics,

Indian Agricultural Research Institute,

New Delhi 110 012, India

³Centre for Sustainable Technology,

Indian Institute of Science,

Bengaluru 560 012, India

*For correspondence.

e-mail: manojfri@gmail.com

Earthquake swarms in Palghar district, Maharashtra, Deccan Volcanic Province

The Palghar district of Maharashtra falls in zone III of the seismic zoning map of India, where earthquakes up to magnitude 6.0 can occur¹. A swarm activity was started in the Palghar district of Maharashtra in November 2018 and is still continuing (till the end of November 2019). According to reports from the National Centre for Seismology (NCS), more than 1,000 earthquakes of micro-to-minor magnitude have occurred in the Dahanu and Talasari talukas of Palghar district, from 3 November 2018 to 15 February 2019. The biggest tremor of magnitude M_L 3.7 was recorded on 1 February 2019, at 3.54 PM (IST). The people of Dahanu and Talasari talukas were panicked by the abnormal ground vibration and burst sound that they felt. In fact, Jawahar city in Palghar district has experienced swarms several times earlier. Another vulnerable region in Maharashtra is Amravati, which witnessed swarm activity in August 2018 (ref. 2). In 1856, the region experienced an earthquake of magnitude 5.7 (Figure

1 a)^{3,4}. The objective of the present study is to provide preliminary information about the ongoing swarm activity immediately after its occurrence. Since the local networks have been deployed a few days after the swarm activity, we attempted to understand the nature of swarm activity, utilizing data from the existing Gujarat seismic network.

The entire study region is almost covered with Deccan traps (Figure 1 b). The major fault in the region is the West Coast Fault (WCF), whose origin is linked to the splitting away of the Indian plate from the Gondwanaland^{5,6}. The Ghod and Upper Godavari are the other faults in the vicinity of Palghar⁷. Further, the lineament/dykes in the region dominantly trend in the N–S and NW–SE directions⁶. The field observations reveal that the lineaments represent fracture zones, shear zones, faults and dykes⁶. The coast parallel Panvel flexure is another major tectonic feature present in the area^{4,6}, along which the Deccan basalts dip to the west, with an increasing

amount of dip. The axial trace of this flexure trends in the NNW direction, parallel to the WCF.

To monitor the seismic activity in and around Gujarat, a dense network (GSNet) of 54 broadband seismographs (BBS) was deployed by the Institute of Seismological Research (ISR)⁸ (Figure 1 a). The seismic data from 45 permanent (online) stations are received via very small aperture terminal (VSAT) at the central station of ISR, in a continuous mode. Among these, one station, Madhuban in Dadra & Nagar Haveli (DNH), is located just north of the region affected by the swarm and four other stations are installed in a stand-alone (offline) mode within 70 km epicentral distance, in Mota Randha (DNH), Kavdej, Limzar and Govani villages of Navasari district, south Gujarat. The data from offline stations are manually collected periodically, once a month. The Guralp CMG-3T broadband sensors and 24-bit Guralp CMG-DM24/REFTEK (RT 130-01) data loggers are installed at all the seismic

stations. For the present analysis, we utilized data from 13 stations of GSNet (blue triangles in Figure 1 *a*) which are located in the proximity of the earthquake swarm region. Initially, we have

located the earthquakes in real-time using the online stations, later we have incorporated the data from nearby offline stations operated by ISR. The detectability of the GSNet is $M \geq 1.6$.

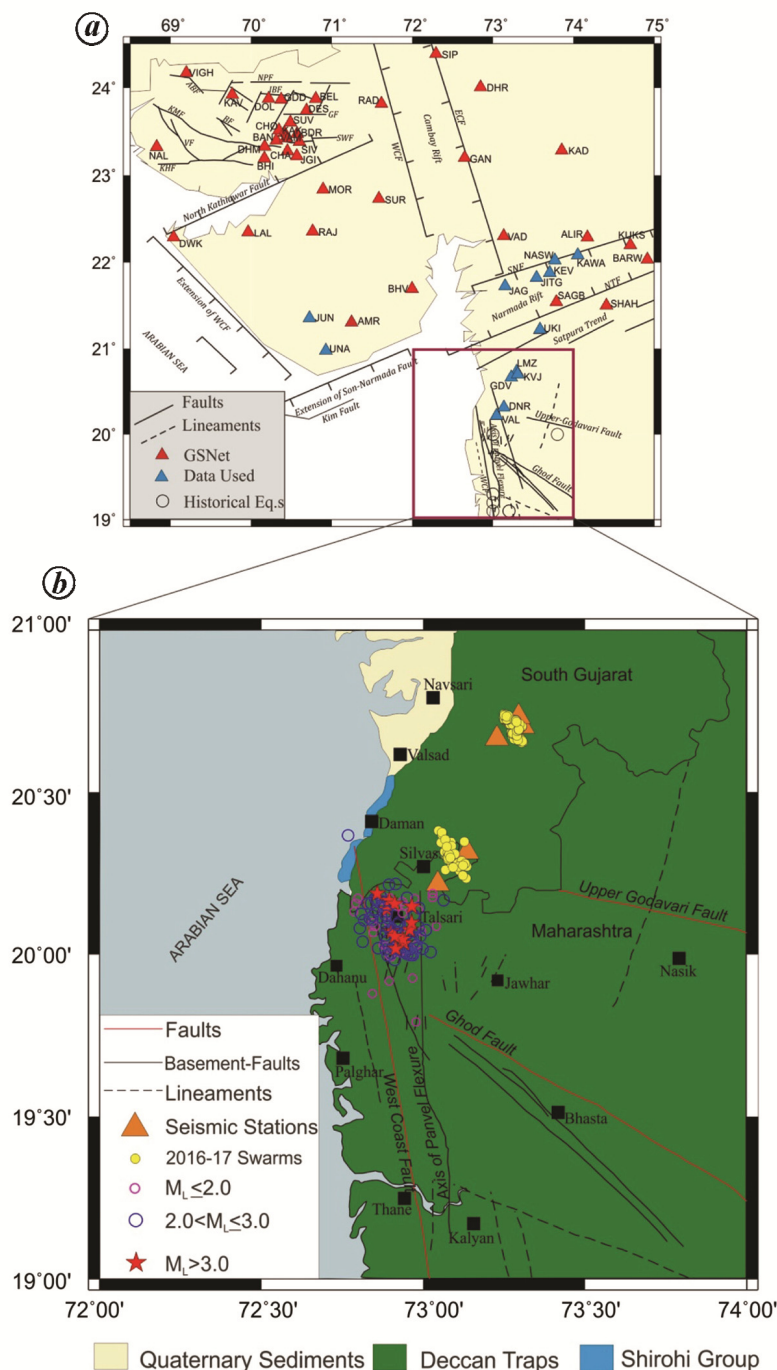


Figure 1. *a*, Regional tectonic map of Gujarat and Maharashtra, western India (modified after Biswas⁵). Locations of historical earthquakes are taken from Chandra³ and Mohan⁴. The study region is marked by a rectangular box. ABF, Allah Bund fault; NPF, Nagar Parkar Fault; IBF, Island Belt Fault; KMF, Kachchh Mainland Fault; KHF, Katrol Hill Fault; GF, Gedi Fault; SWF, South Wagad Fault; NWF, North Wagad Fault; ECF, East Cambay Fault; WCF, West Cambay Fault; SNF, Son Narmada Fault; NTF, North Tapti Fault. *b*, The enlarged geo-tectonic map of the study region with epicentral distribution of earthquakes (open circles and stars) located by the HYPOCENTER program¹⁰.

With the help of the SEISAN earthquake analysis software⁹, the arrival times of P- and S-phases of the earthquake waveforms at various stations were marked manually. The initial earthquake locations were computed using the HYPOCENTER program¹⁰, by considering the 1-D velocity model of the Narmada region¹¹ and an average Vp/Vs ratio of 1.73. A total of 135 events of magnitude (M_L) ranging from 1.6 to 3.7 are located in the Palghar district, from 3 November 2018 to 15 February 2019 (Figure 1 *b*). The focal depths of the majority of shocks are in the range of 2 to 6 km. The average horizontal errors in the initial locations are 3.0 km and 2.7 km in depth. The errors in travel time (RMS values) range between 0.1 and 0.2 sec, for all the events.

The initial swarm hypocentres were further improved by relocating them, using the double-difference earthquake location algorithm (hypoDD)¹² which minimizes error because of unmodelled velocity structure, without the need for station corrections. The detailed methodology of the algorithm is given in ref. 12 and it works on the principle that ‘if hypocentre distance between two earthquakes is small compared to earthquake-station distance and the scale length of velocity heterogeneity, then the ray paths between the source region and a common station are similar along almost the entire ray path’. In such a case the difference in travel-times for two earthquakes observed at a station can be ascribed to the spatial offset between the earthquakes with high precision. During hypoDD inversion, the parameterization was done using the following criteria: (i) the maximum hypocentre distance between earthquake pairs is 4 km, with each earthquake having at least 4 recorded phases, and (ii) the maximum distance between earthquake pairs and the corresponding seismograph station is 300 km. Ninety earthquakes located using both online and offline station data, till 5 February 2019, are only utilized for hypoDD. The epicentral distribution (relocated) of the swarm activity is shown in Figure 2 *a*. In order to interpret their association with the existing lineaments and faults, the epicentres are plotted along a NE-SW cross-section (A-B, in Figure 2 *a*).

We computed the fault plane solution of an earthquake of M_L 3.7 that occurred on 01/02/2019, using the ISOLA code¹³.

The moment tensors are determined using the least-square method. The velocity traces corrected for instrument response were cut from the origin time to 250 sec. Then the traces were passed between 0.07 and 0.22 Hz using a 4-pole band-pass Butterworth filter. The fits between observed and synthetic waveforms at a few stations for the $M_{\text{L}} 3.7$ earthquake are shown in Figure 2 *b*. The focal mechanism indicates a strike-slip fault (Figure 2 *a*). The epicentral distribution clearly shows a NNW–SSE trend. Therefore, we consider the NNW–SSE near vertical plane to be the fault plane.

The distribution of the relocated earthquake reveals that the swarm activity in Palghar follows a general NNW–SSE trend, confined to an area of $10 \text{ km} \times 2 \text{ km}$, which is parallel to the strike of lineaments/dykes/basement faults present in the Panvel Flexure (Figure 2 *a*). The depth distribution of earthquakes that occurred 5 km on either side of the NE–SW profile A–B is shown in the inset of Figure 2 *a*. The depths of most of the earthquakes range between 1.5 and 6.0 km (profile A–B, inset of Figure 2 *a*). It is observed that the hypocentres of swarm earthquakes are on a near vertical plane.

The determined fault plane solution (Figure 2 *a*) shows a strike–slip nature with a near vertical fault plane, sympathetic to the trend of the earthquake epicentres. Nevertheless, previous geological studies and satellite data reveal the presence of lineaments/fractures that are trending NS to NW–SE⁶. Mohan *et al.*⁴ studied the micro-seismicity along the Panvel flexure during 1998–2005 and proposed that the seismicity is due to the reactivation of basement faults in the flexure. It has also shown a cluster of earthquakes in Dhanu, a part of our study region. Recently, a swarm activity was reported just north of the Palghar district¹⁴ in DNH and south Gujarat during September–December 2016 and August 2017–January 2018, immediately after the extended monsoon season, which was ascribed to hydro seismicity.

Swarm-type earthquake sequences have been familiar in Peninsular India and more than hundred examples are reported. It has been observed that majority of the earthquakes in these sequences are localized in space and time, and occurred between June and January, during or soon after the monsoon^{15–17}. However, in view of the continued occurrence of earthquakes even long after the monsoon in Palghar, correlating this swarm activity with monsoon is slightly ambiguous, based on the present analysis. A previous study⁴ has attributed the micro-seismic activity in this region to a tectonically disturbed zone of weakness which developed as a consequence of west-coast rifting, volcanic eruptions and subsequent effects. However, to propose a conclusive mechanism for the swarm activity, geophysical studies like magnetotellurics need to be conducted to image the subsurface structure and identify the depth extent of the lineaments/fractures and faults present in the study region. Also, the rainfall data of the region should be analysed to understand the pore pressure changes and quantify the linkage between rainfall and swarm activity. The focal mechanism solutions are to be determined with data over a wide azimuthal range, to further constrain the tectonics of the region.

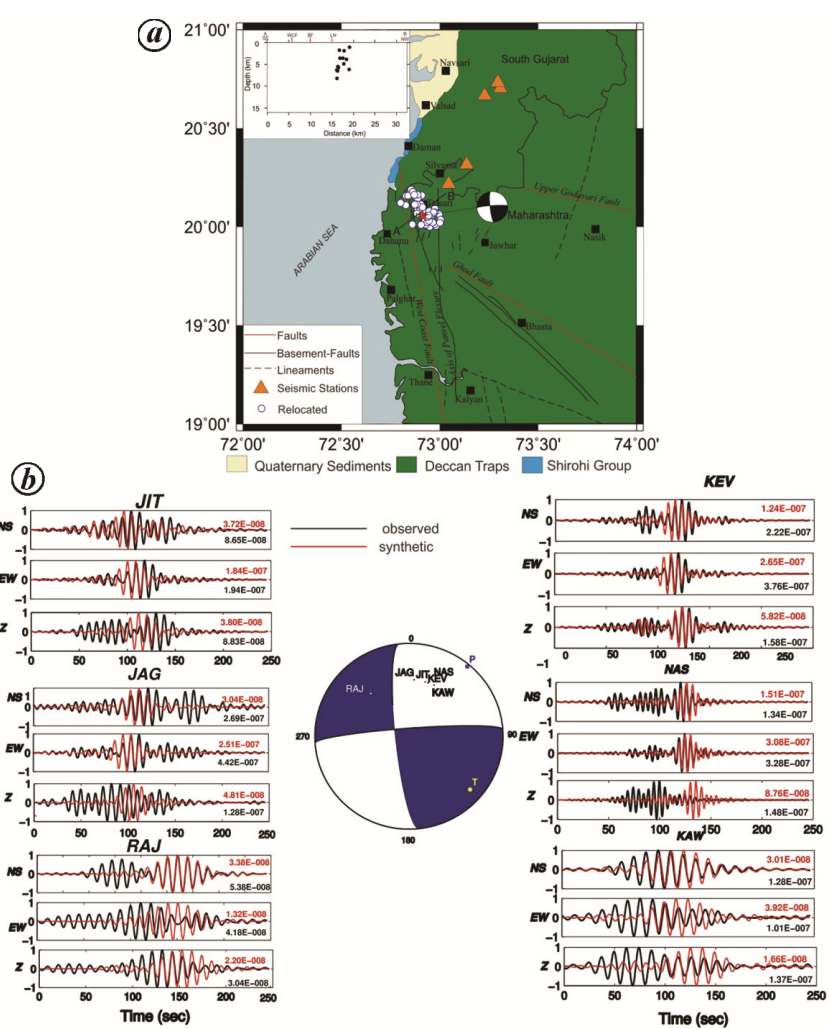


Figure 2. *a*, Epicentral distribution of earthquakes (filled circles) relocated using the double-difference method (hypDD). The fault plane solution of the earthquake of $M_{\text{L}} 3.7$ that occurred on 01/02/2019 is also shown. The A–B line shows the location of SW–NE cross-section user for showing depth distribution of earthquakes. The inset map shows the depth distribution of earthquakes that occurred within 5 km width on either side of the profile A–B. *b*, Waveform match between the observed (black) and the synthetic (red) seismogram at some stations and centroid moment tensor solution of $M_{\text{L}} 3.7$ earthquake used in this study. The normalization factor used for plotting is given for each component at every station for both observed and synthetic seismogram. Y-axis corresponds to displacement (in metre).

1. Bureau of Indian Standards, Criteria for Earthquake Resistant Design of Structures, 2002, fifth revision, p. 39.
2. National Centre for Seismology, Ministry of Earth Sciences, New Delhi;

- <https://www.moes.gov.in/programmes/national-centre-seismology>
3. Chandra, U., *Bull. Seismol. Soc. Am.*, 1977, **67**, 1387–1413.
 4. Mohan, G., Surve, G. and Tiwarari, P. K., *Curr. Sci.*, 2007, **93**, 991–996.
 5. Biswas, S. K., *Tectonophysics*, 1987, **135**, 307–327.
 6. Dessaï, A. G. and Bertrand, H., *Tectonophysics*, 1995, **241**, 165–178.
 7. *Seismotectonic Atlas of India and its Environ*s, Geological Survey of India, Special Publication number, 59, Kolkata, 2000.
 8. Chopra, S. et al., *Seismol. Res. Lett.*, 2008, **79**, 799–808.
 9. Havskov, J. and Ottemoller, L., SEISAN: The Earthquake Analysis Software for Windows, Solaris and Linux, Version 8.0, Institute of Solid Earth Physics, University of Bergen, Bergen, Norway, 2003, pp. 1–400.
 10. Lienert, B. R. E. and Havskov, J., *Seismol. Res. Lett.*, 1995, **66**, 26–36.
 11. Joshi, V., Chopra, S., Mahesh, P. and Kumar, S., *Seismol. Res. Lett.*, 2017; doi:10.1785/0220160203.
 12. Waldhauser, F. and Ellsworth, W. L., *Bull. Seismol. Soc. Am.*, 2000, **90**, 1353–1368.
 13. Sokos, E. N. and Zahradník, J., ISOLA: A Matlab GUI for use with ISOLA fortran codes, USER's Guide, 2000, Ver. 2.5, p. 34.
 14. Sateesh, A., Mahesh, P., Singh, A. P., Kumar, S., Chopra, S. and Ravi Kumar, M., *Environ. Earth Sci.*, 2019, **78**, 381; doi:10.1007/s12665-019-8382-1.
 15. Chopra, S. et al., *J. Geol. Soc. India*, 2008, **72**, 245–252.
 16. Bhattacharya, S. N. and Dattatrayam, R. S., *Gondwana Geol. Magz.*, 2003, v5, 67–85.
 17. Srinagesh, D. et al., *Geol. Soc. India*, 2015, **85**, 419–430.
- Mapping Tools v.4.5.0 (www.soest.hawaii.edu/gmt) was used for preparing the figures.
- Received 21 February 2019; revised accepted 19 December 2019

P. MAHESH^{1,2,*}
A. SATEESH¹
CHARU KAMRA¹
SANTOSH KUMAR¹
SUMER CHOPRA¹
M. RAVI KUMAR¹

¹Institute of Seismological Research,
Raisan,

Gandhinagar 382 009, India

²Present address:

CSIR-National Institute of
Oceanography,
Dona Paula,

Goa 403 004, India

*For correspondence.

e-mail: pmahesh.isr@gmail.com

FORM IV

Particulars of *Current Science*—as per Form IV under the Rule 8 of the Registration of Newspapers (Central) 1956.

- | | |
|---|--|
| 1. Place of Publication: Bengaluru | 4. Publisher's Name, Nationality and Address:
G. Madhavan
Indian
Current Science Association, Bengaluru 560 080 |
| 2. Periodicity of Publication: Fortnightly | 5. Editor's Name, Nationality and Address:
S. K. Satheesh
Indian
Current Science Association, Bengaluru 560 080 |
| 3. Printer's Name and Address:
G. Madhavan
Current Science Association, Bengaluru 560 080 | 6. Name and Address of the owner:
Current Science Association
Bengaluru 560 080 |

I, G. Madhavan, hereby declare that the particulars given above are true to the best of my knowledge.

Bangalore
1 March 2020

(Sd/-)
G. Madhavan
Publisher, *Current Science*